Geologic controls of hydrogen isotope ratios of structural water in serpentinites from San Pedro Limón-Palmar Chico, Tierra Caliente Terrane, Mexico

Delgado-Argote, L.A.[1], I. Casar-Aldrete[2], E. González-Caver[2], P. Morales-Puente[2] and P. Girón-García[3] .
1 Instituto de Geología, UNAM., Present Address: División Ciencias de la Tierra, CICESE, Ensenada,
 Baja California, México.
2 Instituto de Física, UNAM.
3 Instituto de Geología, UNAM.

RESUMEN

El área de San Pedro Limón-Palmar Chico geológicamente se encuentra en el Complejo Tierra Caliente que en esta porción está formado por una secuencia volcanosedimentaria de arco de islas del Albiano-Cenomaniano. De la caracterización de las facies volcánicas y sedimentarias se interpreta la presencia de edificios volcánicos, los cuales definen estructuralmente a pequeñas cuencas donde se depositaron secuencias sedimentarias principalmente clásticas. En San Pedro Limón, un tronco diorítico-peridotítico de 15 km^2 intrusiona principalmente a la secuencia sedimentaria, y pequeñas cuñas de serpentinitas menores de 1 km^2, localizadas hacia el norte de esta zona, se emplazan a lo largo de fallas mayores de orientación N-NW. Se interpreta que el tronco de San Pedro Limón fué emplazado en su posición actual por medio de un mecanismo de torsión durante una deformación transpresiva neogénica. El tronco muestra variaciones petrológicas transicionales desde dioritas (ricas en hornblenda) hasta peridotitas (ricas en clinopiroxeno) con facies intermedias de piroxenitas de hornblenda (ortopiroxeno<10%) y hornblenditas de piroxeno. Nueve muestras de rocas ultramáficas cuyo grado de serpentinización varía entre 10% y 100% fueron analizadas por espectroscopía de radiación infraroja, así como los isótopos de hidrógeno de agua estructural de las serpentinitas y de una muestra de crisotilo. Los espectros de infrarojo indican la presencia de lizardita y crisotilo (serpentinas de baja temperatura) y ausencia de antigorita (serpentina de alta temperatura). Los valores de δD del agua estructural varían entre -85 y -116 por mil, lo que indica inequívocamente un origen meteórico. Además, se observó que los valores de δD son más negativos conforme es más intensa la serpentinización. Se interpreta que ésta se efectuó en asociación con procesos cinéticos a bajas temperaturas, más que en equilibrio con el agua meteórica local. La fase principal de serpentinización está asociada con el régimen tectónico transpresivo y se efectuó de manera simultánea al emplazamiento mecánico de los intrusivos, el cual desarrolló condiciones locales de hidrotermalismo.

PALABRAS CLAVE: Isótopos de hidrógeno, serpentinita, Cretácico, espectroscopía de infrarojo, área de San Pedro Limón-Palmar Chico, Complejo de Tierra Caliente.

ABSTRACT

The area of San Pedro Limón-Palmar Chico is geologically located in the Tierra Caliente Complex. The complex is composed of an Albian-Cenomanian volcanosedimentary sequence of island arc type. A series of volcanic edifices is interpreted from the features of volcanic and sedimentary facies. The sedimentary sequences (mainly clastic) were deposited in small basins, structurally controlled by the volcanoes. In San Pedro Limón, a 15 km^2 dioritic to peridotitic stock intrudes mainly the sedimentary sequence, whereas small wedges of serpentinites not larger than 1 km^2 are emplaced along N-NW structural trends. The San Pedro Limón stock is interpreted as having been emplaced by a torsion mechanism during a Neogene transpressive disturbance. The stock shows a transitional petrographic variation from hornblende-rich diorites to clinopyroxene-rich peridotites with intermediate hornblende pyroxenite (orthopyroxene<10%) and pyroxene hornblendite facies. Nine ultramafic samples, ranging from 10% to 100% serpentinization, were analyzed by infrared spectroscopy. Only low-temperature serpentines such as lizardite and chrysotile were identified. Hydrogen isotopic ratios were determined on structural water from nine serpentinites and one sample of chrysotile. δD ranges from -85 to -116 per mil, which unequivocally indicates a meteoric origin. Furthermore, the δD values decrease with increasing degree of serpentinization. The serpentinization must have occurred at low temperature under kinetic conditions. The main serpentinization phase is associated with a tectonic transpressive regime, and occurred simultaneously with the mechanical emplacement of intrusives which developed local hydrothermal conditions.

KEY WORDS: Hydrogen isotopes, serpentinite, Cretaceous, infrared spectroscopy, San Pedro Limón-Palmar Chicho, Tierra Caliente Complex.

INTRODUCTION

The ultramafic rocks of southern Mexico have been mainly documented as part of terranes of volcanic arc affinity (Delgado-Argote, 1986). These magmatic arcs are mainly andesitic in composition and the ultramafics are generally serpentinized. Their emplacement can be related to severe compressive deformations featuring low-angle thrust faults (Oaxaca; Delgado-Argote, 1989) or to subvertical diapiric-like intrusions (Guerrero; Delgado-Argote, 1986 and Delgado-Argote *et al*, 1986). In contrast, the San Pedro Limón stock, in the southern part of the State of

Mexico (Figure 1), shows a minor degree of serpentinization and therefore its structural behavior is more rigid than for the ultramafics of Guerrero and Oaxaca. Such a low degree of serpentinization suggests magmatic differentiation trends in transitional associations of peridotitic to dioritic rocks (Delgado-Argote *et al*, 1988).

The purpose of this work is to establish a correlation of hydrogen isotopic variations with respect to mineralogy and grade of serpentinization of the ultramafic masses in the San Pedro Limón-Palmar Chico area, as well as to determine the "type" of water involved in the alteration process.

Based upon the isotopic compositional range of oxygen and hydrogen, five types of natural waters have been recognized (Sheppard, 1986). Barnes and O'Neil (1969), Wenner and Taylor (1973 and 1974), and Magaritz and Taylor (1974) have shown the presence of meteoric, magmatic and metamorphic waters within the serpentine structure. They found a good correlation between the type of water and the formation temperatures of different serpentines. Thus, high-temperature (~300°C) antigorite is correlated with metamorphic water, while low-temperature chrysotile and lizardite (~100°-200°C) incorporate meteoric water (Wenner and Taylor, 1974).

The ultramafic rocks analyzed in this paper show different degrees of serpentinization (10 to 100%). This variation depends on different factors: composition of the protolith, location in the stock, and relationship with respect to major structural features (mainly strike-slip faults). Sampling localities are shown in Figure 2. Size and composition of the different bodies are as follows: San Pedro Limón, 15 Km^2 of hornblendites, pyroxenites, and serpentinites; Palmar Chico, 0.9 Km^2 of clinopyroxenites and serpentinites; Huistitla, 0.5 Km^2 of serpentinites; La Esmeralda, 0.1 Km^2 of serpentinites.

ANALYTICAL METHODS

The samples of serpentinized ultramafic rocks were analyzed by the infrared absorption technique. Potassium bromide pellets containing 0.75% of mineral for the region between 4000-2000 cm^{-1}, and 0.50% of mineral for the region 2000-400 cm^{-1} were prepared by standard techniques (Brindley and Zussman, 1959). The analyses were performed with a Perkin-Elmer spectrometer Model 783, at the Instituto de Geología, UNAM.

The hydrogen isotope analysis on the serpentinites consisted of three steps: complete and non-fractional extraction of the water, water reduction, and isotopic analysis of the produced hydrogen. The samples were ground to a very fine powder (150-200 mesh). Prior to water extraction, the sample powders were baked at 200°C for about 24 hours. Samples of approximately 200 mg in weight were transferred to a clean quartz tube and connected to a vacuum line. The serpentinites were outgassed for one hour and surface water was eliminated by heating the sam-

ple to 200°C with a Cu-block for an hour longer. The temperature was then raised to above 700°C and maintained for 60 minutes (See Table 1). The evolving water (typically about 10μl) was condensed in a LN$_2$ cold trap. Other gases were pumped out. When the vacuum loss was greater than 1 Torr, no reduction of water was performed. The condensed water was heated and then reduced over metallic uranium at 950°C, and the hydrogen was pumped into a glass flask with a Topler pump. The deuterium-hydrogen ratios were determined in the hydrogen gas using a Finnigan MAT-250.

All the samples processed were analyzed in duplicate or triplicate. The results of the replicates were in agreement within ± 2.0 units for 95% of the samples. The deuterium analyses are reported using Delta notation, as defined by Craig (1961), and SMOW (Standard Mean Ocean Water) as a standard.

$$\delta D = \frac{(D/H)sample - (D/H)smow}{(D/H)smow} \times 1000$$

GEOLOGIC FRAMEWORK

The area of San Pedro Limón-Palmar Chico is located in the southern part of the State of Mexico (Figure 1), where 270 Km^2 of detailed mapping was conducted. In this region, an Albian-Cenomanian volcanosedimentary sequence has been described (de Cserna, 1982), belonging to the Tierra Caliente Complex (Ortega-Gutiérrez, 1981). References about ultramafic rocks in this area are scarce. García-Calderón (1978) reported some geological features related to serpentinites in Palmar Chico (San Francisco Los Pinzanes), while Salas-Castellanos (1982) refers to the presence of "ultrabasic phases" (pyroxenites) in the eastern portion of San Pedro Limón (called Tronco de Alambique by de Cserna, 1982).

The volcanosedimentary sequence is affected by intrusive rocks whose composition and geometry ranges from diorites to peridotites, and from dikes to stocks. We divide the volcanosedimentary sequence in two main domains depending on the relative amount of sedimentary rocks over crystalline volcanics. A simplified geologic map of the area is shown in Figure 2. The volcanic domain consists mainly of lava flows, a sedimentary domain is represented by immature sediments, and the intrusive bodies are dioritic to periodotic rocks.

As for the age of the sequence, the volcanic domain is correlated with the Xochipala Fm., and the sedimentary rocks with the Arcelia Fm., of roughly Cenomanian-Coniacian age (de Cserna, 1982). Salas-Castellanos (1982) identified the Xochipala Fm., but correlates a sequence of pillowed lavas and interstratified wackes, black shales and minor limestones with the Cenomanian-Turonian Mal Paso Fm., of Huetamo (Pantoja-Alor, 1959). Nevertheless, the maximum age of the sequence referred for the Xochipala Fm. (upper and lower members; de Cserna, 1982) can be Early Cretaceous (Pantoja-Alor, 1983). With respect to the ultramafic rocks, it is assumed that they are ge-
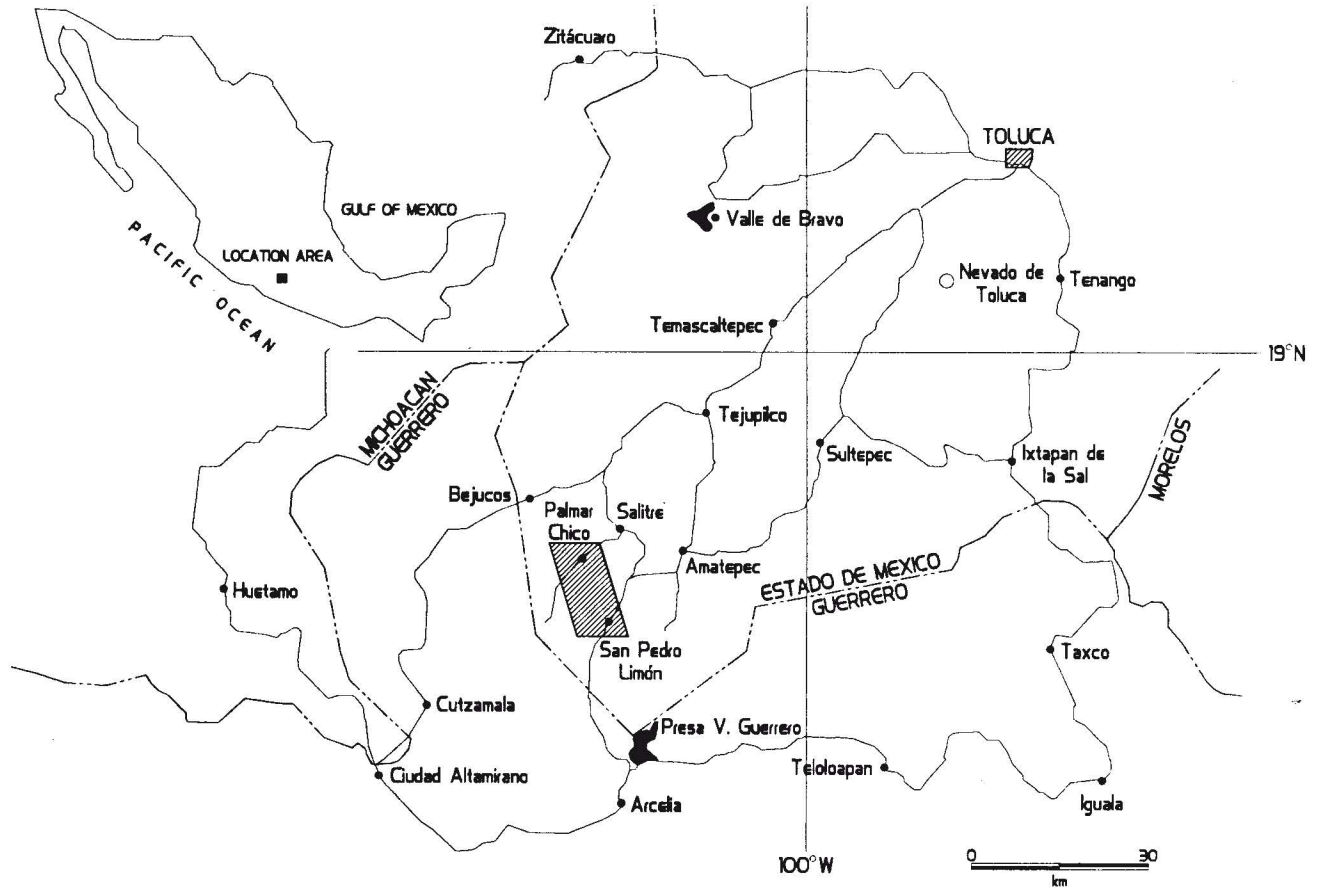
Fig. 1. Location map indicating in grid pattern the area of geologic map.

Table 1

Experimental conditions for isotope analyses of hydrogen.

#	SAMPLE	WEIGHT (mg)	TEMP (°C)	TIME (min)	δD ‰	AVG. %	S.D.	MAX. DIF.
1	ME-V-3	100 100 100	615 754 673	60 51 60	-107.09 -109.60 -110.93	-109	±1.95	3.84
2	ME-V-4	214.5 200	759 718	60 60	-86.49 -84.10	-85	±1.69	2.39
3	ME-V-5	105 100	728 723	60 60	-104.77 -114.02	-109	±6.54	9.25
4	ME-V-13	100	686	40	-110.93	-111		
5	ME-V-7	100 100	686 702	45 45	-116.45 -116.08	-116	±0.26	0.37
6	29-M-88	100 100	716 725	60 60	-103.10 -102.43	-103	±0.47	0.67
7	29-M-88	153	780	60	-109.95	-110		
8	25-M-88	100 100 100	766 759 737	67 60 65	-107.43 -102.28 -102.61	-104	±2.88	5.15
9	19-M-88	102 103	692 764	60 60	-101.10 -94.34	-98	±4.78	6.76
10	34-M-88	100 100	788 649	60 60	-104.05 -106.65	-105	±1.84	2.76

Note: Sample 7 is pure chrysotile from veinlets of sample 29-M-88
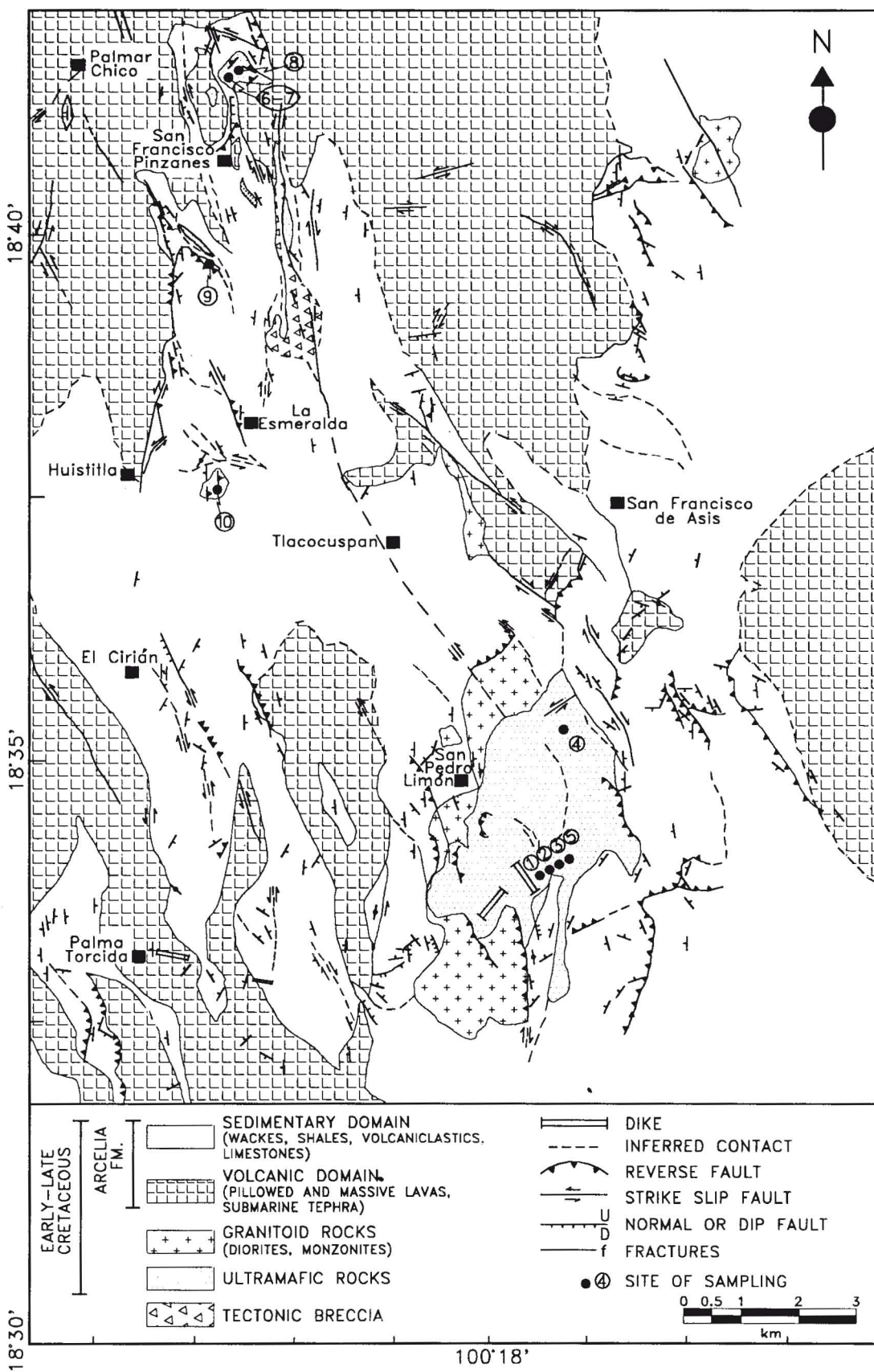
417

Fig. 2. Generalized geologic map of the area of San Pedro Limón-Palmar Chico, State of Mexico.

netically related to the dioritic intrusives and therefore should be contemporaneous (Delgado-Argote *et al.*, 1988). The stock of San Pedro Limón (El Alambique) was compositionally classified by de Cserna (1982) as quartz-monzonitic, and magmatically associated to the stock of Tlatlaya located eastward. The age of this stock had been interpreted to be Santonian based on a K-Ar date obtained from a fuchsite sample of the Esquisto Taxco Fm., (79±5 Ma; Fries and Rincón-Orta, 1965, *in* de Cserna, 1982). This mica is considered to have been reset during a thermal event associated with the emplacement of the nearby intrusives. If this interpretation is correct, a close temporal correlation also exists between the intrusives and the whole volcanosedimentary sequence.

The volcanic domain is composed of thick and widespread submarine andesitic lava flows and volcaniclastics, and a smaller amount of subaereal tuffs. These tuffs are inferred to have been deposited in small internal basins and, due to their close association with sandstones and shales, they are considered as part of the sedimentary sequence in this work. The main structures in the volcanic domain are pillowed and massive flows, small feeder dikes, autobrecciated lavas, hyaloclastites and submarine tephra. Most of the pillowed and autobrecciated lavas include limestones and other clastic sedimentary rocks between individual pillows or mixed in the breccia matrix. The composition of lavic material is dominantly andesitic (An<50), showing a similar mode to the diorites (Figure 3). Geometrically, the recognition of proximal deposits defines the presence of volcanic edifices which control the distribution of sediments along local sedimentary basins (for example, Cerros La Onza). From their clastic association and the presence of interlayered lava flows in the sedimentary domain, such basins are considered to be unstable (Delgado-Argote *et al.*, 1988). In addition, in the northern portion of the area (Palmar Chico), the sedimentary domain shows a greater pelitic composition than the mostly psamitic tendency of the area of San Pedro Limón.

The general structure of the area of San Pedro Limón-Palmar Chico is dominated by features associated with transpressive deformation of probable neogenic age, as red beds of the Balsas Formation are affected by strike-slip faulting. This structural disturbance features dominantly left-lateral faulting, trending N 32°W to N 07°E. Depending upon the rock type, the larger structures have an average width of 50m or less, and develop tectonic melanges and narrow mylonitic zones. The 500 m-wide La Esmeralda fault is an important exception; its maximum amplitude is found at Cerro La Esmeralda, where many small reverse faults developed in association with "palm tree"-like structures (Sylvester, 1988). The ultramafic body of Palmar Chico is located in the northern part of the Esmeralda Fault, which is bifurcated, and the intrusive is emplaced on the inside and shows a plastic-rigid behavior related to partial serpentinization. The intrusion mechanism is probably torsion in a compressive regime, as observed at San Pedro Limón. To the eastern side of this stock, a sequence dominated by soft carbonaceous shales and minor graywackes
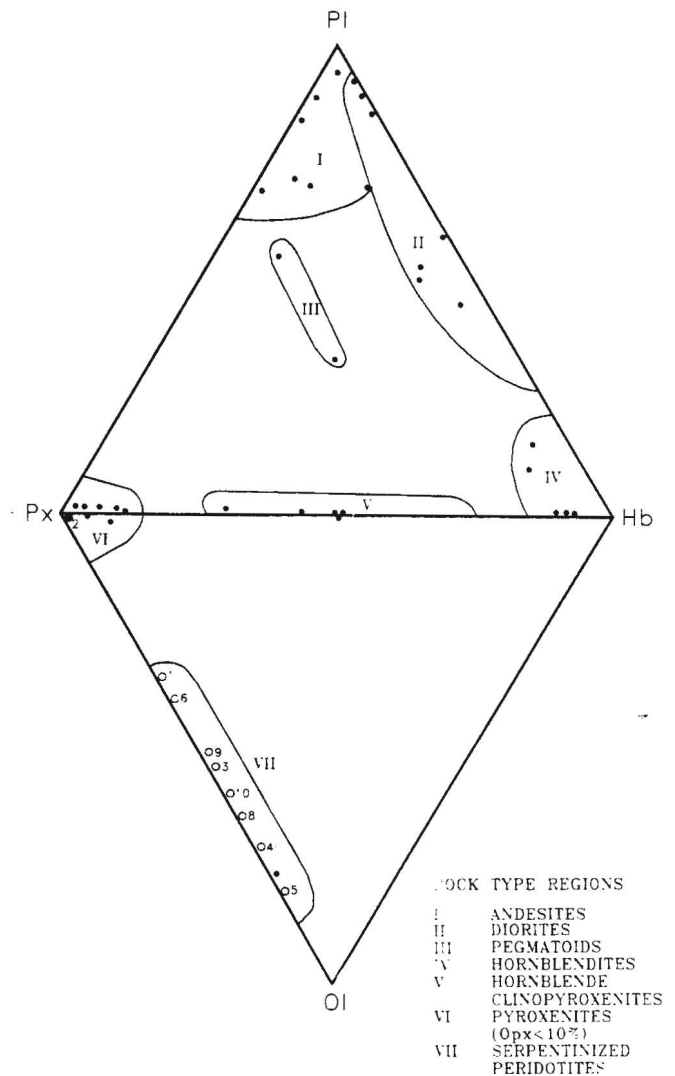

Fig. 3. Double triangle Ol-Px-Hb-Plg of crystalline rocks. Modal content of highly serpentinized periodotites was inferred from the presence of bastites (after orthopyroxene) and concentration of secondary magnetite, estimated to derive mostly from olivine.

and lavas is affected by reverse faults with small displacement. They are associated with transcurrent faults and the presence of the rigid crystalline stock (Figure 2). In a previous work (Delgado-Argote, 1987), the emplacement of the stock was interpreted as due to mechanical torsion during the Neogene transpressive disturbance. Geometrically, it is important to notice that reverse faulting roughly follows the periphery of the stock (Figure 2).

A wide N 20°W oriented anticlinorium located in the central part of the area was defined from the solution of 140 strata poles. By a careful treatment of the structural data, small synclines and anticlines, mainly in the Palmar Chico-La Esmeralda area (Figure 2) can be detected. These folded structures characterize the regional tectonic regime which is related to Neogene left-hand strike-slip faulting.

INTERNAL GEOLOGY OF THE
ULTRAMAFIC BODIES

Except for the San Pedro Limón stock, the ultramafic bodies of Palmar Chico, La Esmeralda, and Huistitla are clearly related to large lateral faults. The ultramafics are in tectonic contact with sedimentary rocks, and the most prominent feature of the three minor bodies is the development of shearing structures in serpentinites. Inside the body of Palmar Chico, some original cumulitic textures were preserved between shearing planes. The contacts with respect to the country rocks tend to be vertical, except for the serpentinitic wedge of La Esmeralda which is emplaced along a reverse fault. The small ultramafic bodies are interpreted to be portions of the top of larger stocks.

In the double triangle Ol-Px-Hbl-Pl (Figure 3), the petrographic analyses of 49 intrusive rocks (41 from San Pedro Limón), are plotted. Transitional modes between lherzolites (?), wehrlites (?), pyroxenites, hornblende pyroxenites, hornblendites, and diorites are shown. Dominant textures in the ultramafics are cumulitic, pegmatoid, brecciated (by emplacement), and sheared by plastic flow (serpentinites). Dioritic rocks are predominantly granular seriated, and are often anisotropic. Modes were calculated from volume-percent estimation diagrams, and modal composition of some peridotites (lherzolites and wehrlites), were inferred from the presence of bastites (after orthopyroxenes) as well as secondary magnetite in serpentine minerals. Magnetite is believed to be mostly derived from olivine (Page, 1968; Coleman, 1971; Wicks and Whittaker, 1977). The details of the petrographic data will be discussed in a forthcoming paper on the geology and petrology of the ultramafics of San Pedro Limón-Palmar Chico area.

The general structure of the San Pedro Limón stock is internally dominated by reverse and left-hand strike-slip faults, fractures, and dikes showing a vertical tendency. In Figure 2, penetrating strike-slip faults are indicated in such a way that at least two generations of structures are in evidence. Both of them may be closely related to the history of the stock emplacement.

The San Pedro-Limón composite stock is surrounded by sedimentary rocks and the contacts are sharp and mainly tectonic. Chilled margins are absent; and plastically deformed rocks, slickensides and unchanged grain size in diorites testify to a mechanical intrusion. Internal contact relationships between the dioritic and ultramafic rocks are quite different. They can be described as border zones, especially in the southern part of the stock, where clinopyroxene-rich pegmatoids in diorites gradually change to clinopyroxenites. This zone shows a strong deformation due to lateral faulting, yet most contacts between mafic and ultramafic rocks are gradational in composition suggesting a vertical forced emplacement. Dioritic and andesitic dikes intrude the central parts of the ultramafic mass; they are melanocratic and frequently associated to fractures or faults. Besides the vertical tendency of most of the internal structures in plan view, they are mostly curvilinear. Along Alambique Creek, small protruding domes about 10 m in diameter are common in ultramafic rocks. Such small local structures are believed to reflect the general style of emplacement, as suggested by the curvilinear faults and the geometry of perpendicular dikes and fracturing (Figure 2). In contrast with the ultramafic units, where doming and horizontal fracturing are present, mineralogical anisotropy in diorites, and foliation in serpentinized rocks, show a subvertical tendency, particularly along the contacts.

As summarized in Table 1, internal fabrics such as autobrecciation and development of cumulitic and related textures are observed in hand specimens and on the microscopic scale as well.

DESCRIPTION OF SERPENTINIZED
ULTRAMAFIC ROCKS

The intrusive ultramafic rocks are gradational in terms of intensity of serpentinization. In San Pedro Limón, the average degree of serpentinization is 50%, while in the smaller bodies the degree of serpentinization can be as high as 100%. The content of primary and secondary minerals is summarized in Table 2, and a proposed classification of the respective protolith is shown. Four out of five selected samples from San Pedro Limón belong to a broad wedge of ultramafics showing a varied mineralogy (Figure 3 and Table 2; samples 1,2,3, and 5). Sampling was carried out normal to the strike of emplacement in a 100 m wide section, where plastic to rigid rocks are present. This section is representative of the style of intrusion and ultramafic composition of the whole mass of San Pedro Limón. Sample 5 is located in the northern part of the stock, and belongs to a single ultramafic body intruding a larger mass of horblendites and clinopyroxenites. In this area, serpentinization is estimated to be almost complete (up to 80%). Depending upon the protolith composition, in most cases, the serpentinization degree is proportional to the concentration of small veins of secondary magnetite per area ($d = \Sigma l/A$; where d is concentration of veinlets, Σl is the total length of veinlets and A is the measured area) (See Table 2). Serpentine minerals are primarily correlated with textures following the criteria given by Wicks and Whittaker (1977). Different degrees and types of serpentinization related to hydrothermal alteration can be observed. This depended on mineralogy and spatial association with respect to large structures where intense shearing stress predominated. Most of the observed textures in thin section are pseudomorphic, non-pseudomorphic, and veins (Table 2). Pseudomorphic textures include the presence of bastites (after orthopyroxene), mesh textures after olivines, and serpentine rims in zones of selective alteration. Lizardite seems to be the main serpentine mineral. Non-pseudomorphic textures are both interlocking and interpenetrating textures of lizardite. Some antigorite in association with chlorite seems to be present in sample ME-V-13, but is not confirmed by infrared spectra (Figure 4). There are two kinds of serpentines formed in veins: slip-fiber chrysotile developed by shearing stress during the emplacement of

Table 2

Petrographic summary of ultramafic rocks from San Pedro Limón-Palmar Chico.

#	SAMPLE	LOCALITY	MINERALOGY PRIMARY						SECONDARY					TEXTURE	CLASSIFICATION	REMARKS
			Ol	Op	Cp	Hb	Ox	S	Ox	A	U	Cl	Ep			
1	ME-V-3	ALCANT	·	·	Ø	X	·	Ø	·	·	O	/	/	ADCUMULITIC	WEHRLITE	Hbl-Cpx exsolutions. Strong shearing (S~40%)
2	ME-V-4	ALCANT	·	+	□	·	·	X	·	+	+	+	·	ADCUMULITIC	CLINOPYROXENITE	2 px in poikilitic relation. Selective alteration (S~10%)
3	ME-V-5	ALCANT	/	/	O	·	/	□	X	·	·	·	·	GRANULAR CUMULITIC	LHERZOLITE	Lizardite bastites and veinlets of chrysotile (S~70%)
4	ME-V-13	FABRICA	·	/	/	·	/	□	+	/	·	+	·	SECONDARY SHEARING	SERPENTINITE (LHERZOLITE?)	Very high secondary magnetite in veinlets -d>0.8 (S~80%)
5	ME-V-7	ALCANT	·	·	·	·	/	□	X	·	·	·	·	SECONDARY SHEARING	SERPENTINITE	Very high secondary magnetite in veinlets -d>2 (S~100%)
6	ME-29-M	PALMAR CHICO	·	·	·	·	/	□	X	/	·	·	/	CUMULITIC	SERPENTINITE (WEHRLITE)	Abundant chrysotile veinlets. Cpx bastites (S~75%)
7	ME-29-M	PALMAR CHICO	·	·	·	·	·	□	·	·	·	·	·	VEINS	SERPENTINITE (WEHRLITE)	Sample taken from cross fiber chrysotile veins.
8	ME-25-M	PALMAR CHICO	·	/	·	·	/	□	X	·	·	·	·	CUMULITIC	SERPENTINITE (LHERZOLITE)	Opx bastites. Chrysotile along shearing planes and stockwork veinlets (S~80%)
9	ME-19-M	ESMERALDA	·	·	·	·	/	□	X	/	·	·	·	SECONDARY SHEARING	SERPENTINITE	Chrysotile stockwork. Pseudomorphic amphiboles after cpx (?) (S~90%)
10	ME-34-M	HUISTITLA	·	·	·	·	/	□	X	/	·	·	·	INTERCUMULITIC(?)	SERPENTINITE (LHERZOLITE?)	Opx (?)-cpx bastites (S~95%)

Minerals: Ol = Olivine, Op = Orthopyroxene, Cp = Clinopyroxene, Hb = Horblende, Ox = Oxides, S = Serpentine, A = Actinolite-tremolite, U = Uralite, Ep = Epidote, Cl = Chlorite.

Abundances: - = Absent or traces, / = 1-5%, + = 5-10%, X = 10-20%, O = 20-35%, Ø = 35-50%, □ > 50%.

Observations: First five samples belong to the stock of San Pedro Limon (ALCANT = Alcantarilla).
S~70% = Volume percent serpentine minerals approximates degree of serpentinization used in Figure 7. d>2 = Density of magnetite veins after d = Sum of veinlets lenght per area. Both, S and d are taken as representative of each sampling site and no error estimation was done.

the ultramafic mass, and cross-fiber chrysotile showing a perpendicular or oblique arrangement with respect to the direction of emplacement cutting primary minerals. In both cases, chrysotile is the latest of at least two episodes of serpentine generation, and its identification is unequivocal. By contrast, lizardite and antigorite cannot be identified from each other in most non-pseudomorphic textures.

Primary textures inferred from the presence of bastites and primary minerals are mainly cumulitic; they seem to be fine-to medium-grained mesocumulates. Coarse-grained ultramafics often show an equigranular tendency, and intergrowth textures are commonly observed in pyroxene-rich rocks. As to the compositional variation of the San Pedro Limón stock, in the double-triangle Ol-Px-Hbl-Pl (Figure 3), olivine-rich ultramafics lack hornblende whereas, in plagioclase-rich rocks, pyroxenes are concentrated in a low proportion with respect to the amphibole. As a whole, hornblende pyroxenites and pyroxene hornblendites are volumetrically more important in the San Pedro Limón stock. The presence of hornblende in pyroxenites and its absence in peridotites suggests that water plays an important role after the earlier formation and concentration of the olivine-rich ultramafics. However, it is not easy to tell some uralite from primary hornblende in the hydrothermally altered specimens. On the other hand, orthopyroxenes are concentrated mainly in pyroxenites in proportions of less than 10% of total volume content (region V, Figure 3). As seen in Figure 3, the modal distribution strongly suggests a crystallization path following the Ol-Px-Hbl-Plg mineral vertices.

As for the presence of orthopyroxene, Wager and Deer (1939; cited in Cox *et al*, 1979) reported that in the Skaergaard intrusion, parts of the border group contain primary orthopyroxene, which is replaced by orthopyroxene inverted from pigeonite in the rocks of the layered series of the intrusion. From the presence of primary orthopyroxene in the quickly cooled rocks, they deduced that this mineral might be a significant phase in the unexposed

layered rocks presumed to form the lower parts of the intrusion. In the southernmost part of the San Pedro Limón area, a similar situation may arise since orthopyroxene is only observed near marginal zones and in portions of pegmatoid-rich diorites. Besides, sample ME-V-4 apparently shows exsolution-like textures of clinopyroxene from orthopyroxene, much as described in Cox *et al* (1979).

SERPENTINITES AND SERPENTINIZATION

The main textures of serpentinized rocks are briefly described in Table 2. One problem to solve regarding the chemical and physical characteristics of serpentines is the identification of individual serpentines. From the three main types of serpentines, in most cases, chrysotile can be easily identified with the petrographic microscope but most of the analyzed samples show non-pseudomorphic textures, and textural criteria are not sufficient to tell antigorite from lizardite. These minerals are so similar, and occur in both interlocking and interpenetrating textures, that they cannot be recognized from each other. Antigorite is a high-temperature serpentine (~300°C) while chrysotile and lizardite form in low-temperature regimes (less than 200°C). The assumed temperatures are based upon $^{18}O/^{16}O$ fractionation measured on magnetite-serpentine pairs formed under isotopic equilibrium (Wenner and Taylor, 1974), and δD fractionation factors between clinochrysotile and water, experimentally determined by Sakai and Tsutsumi (1978). The absence of high-temperature serpentine (antigorite) is important in order to assure that no fractionation was produced during the recovery of structural water in the laboratory. Antigorite is assumed to be derived from low-temperature serpentines during prograde metamorphism at about 300° to 400°C, under limited availability of water (Wenner and Taylor, 1974; Wicks and Whittaker, 1977; Sakai and Tsutsumi, 1978).

The infrared spectra of the nine ultramafic samples are given in Figure 4 together with selected serpentine spectra. Five samples come from the San Pedro Limón stock and
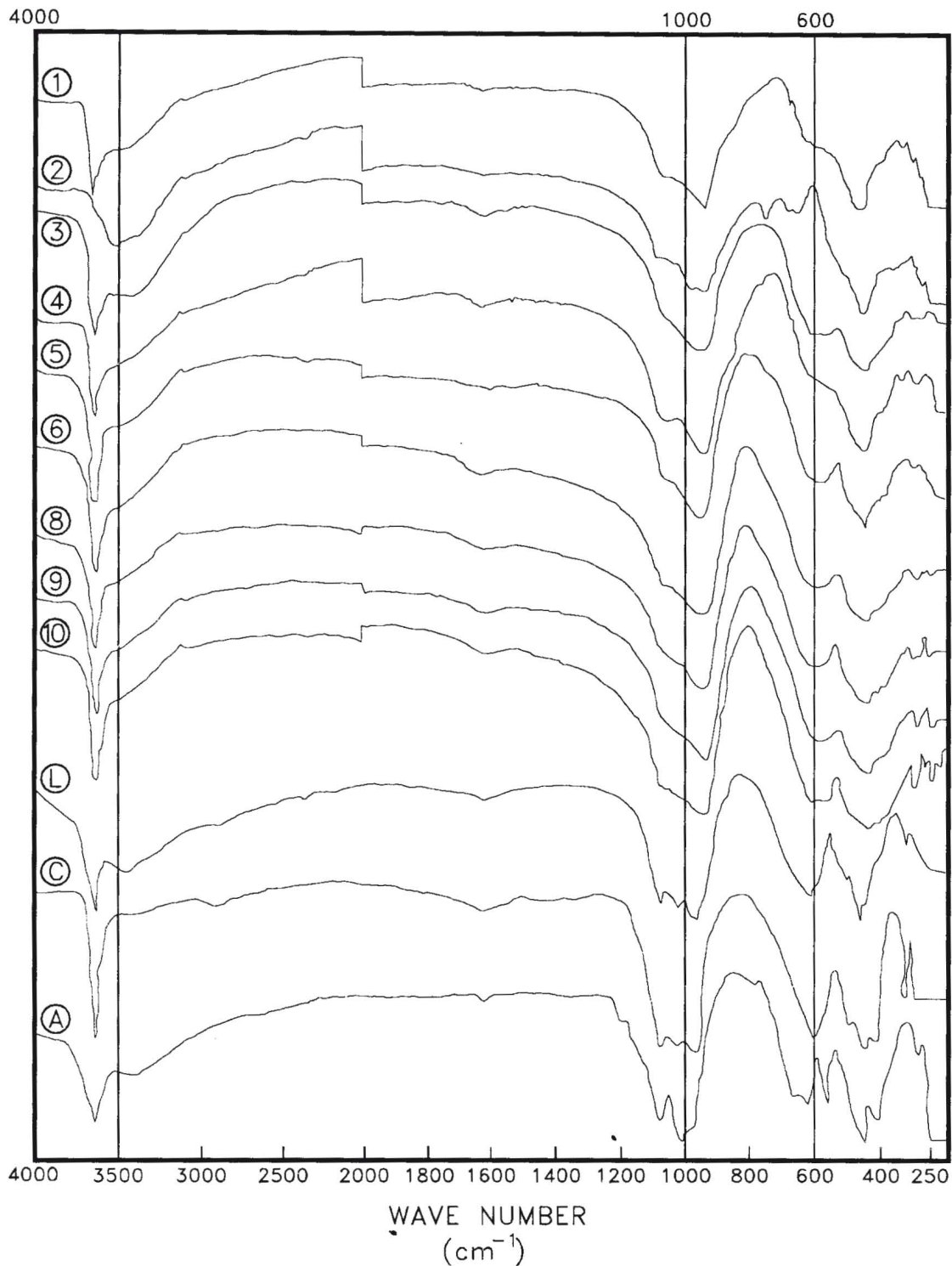
Fig. 4. Infrared spectroscopy of nine serpentinites (see Table 2 for petrographic description). The spectra of lizardite (L), chrysotile (C) and antigorite (A) after Luce (1971) are included for reference. Notice the sharp band at 570 cm^{-1} of antigorite.

four are from Palmar Chico. It has been recognized that the spectrum of antigorite is distinct from that of lizardite-chrysotile. Luce (1971) reported that the key band for antigorite is 450-453 cm^{-1} Furthermore, the absence of a sharp band at 570 cm^{-1}, characteristic of antigorite (Yariv and Heller-Kallai, 1975), allows us to confirm that our samples are antigorite-free. According to Luce (1971) most authors conclude that infrared spectra cannot distinguish between lizardite and chrysotile in a mixture. The broadening of the bands observed in Figure 4 can be explained as due to inhomogeneities in the chemical composition of serpentines (Yariv and Heller-Kallai, 1975; Golightly and

Arancibia, 1979). For our samples, the powders were prepared from whole rocks showing variable degree of serpentinization.

In San Pedro Limón, selective hydrothermal alteration is widespread in both country and intrusive rocks, and metamorphic facies and textures are mostly absent beyond the faulting zones. We assume that partial serpentinization took place under hydrothermal conditions and that the association lizardite-chrysotile was initially formed before the general structural disturbance. In Palmar Chico, La Esmeralda, and Huistitla a second generation of chrysotile was developed, imprinting foliated non-pseudomorphic textures. This second generation of serpentines is also found in some peripheral zones of San Pedro Limón and can be related to the mechanical effect of intrusion.

D/H ISOTOPE DATA AND VARIATIONS

The δD values of ten selected samples from serpentinized ultramafics of San Pedro Limón-Palmar Chico vary between -116 and -85 per thousand relative to SMOW, depending on the degree of serpentinization and composition of the protolith. In tables I and II, the general petrographic characteristics and results of the isotopic analyses are shown. Except for samples 3 and 9, the range of δD values for duplicate analyses was less than 6 per mil, and most of them are within the experimental range of 2-3 per mil; therefore, our procedure of extraction of structural water is believed to be correct.

Wenner and Taylor (1974) found a good regional correspondence between δD values of serpentines, latitude and local meteoric water. Sakai and Tsutsumi (1978), from analyses of meteoric waters and serpentinites from Japan islands (from 45° to 30°N) also found that the latitude-δD correlation holds. We have found that the absence of meteoric water analyses makes it difficult to establish a correlation of this kind. In general, for the three regions of Mexico, some correspondence may exist with respect to latitude; but when compared with the map of general variation in δD of today's meteoric waters in North America (Wenner and Taylor, 1974), the values of highly serpentinized rocks are very low (Figure 5). In the State of Mexico, the values of δD in meteoric waters should be in the range of -50 to -70 per mil. Combining the empirical equation $\delta D = 5.6ta-100$ per mil (Dansgaard, 1964; cited *in* Sakai and Tsutsumi, 1978) with the annual mean air temperature for the State of Mexico, which is 27.3°C (Secretaría de Programación y Presupuesto), yields an approximate δD of -53 per mil for local modern meteoric waters. More analysis is necessary; but Figure 5 shows a good δD-latitude correlation for Oaxaca, Guanajuato, and the State of Mexico (Casar-Alderete *et al,* 1986). If this correlation is correct, we may assume that the structural water of the analyzed serpentines is of meteoric origin. Hydrogen is not temperature dependent, and the δD values turn out to be lower than values of magmatic or metamorphic waters (Sheppard, 1986). Our isotope data fit better the rock composition shown in Table 2 and, in consequence, the degree of serpentinization. From the petrographic description of Table 2, in Figures 6a and 6b, we

compared the variations of δD to serpentinization and the inferred ultramafic protolith. As expected, olivine-rich rocks present more intense serpentinization than pyroxene-rich ultramafics. Also, more strongly serpentinized rocks show lower δD values when they belong to the same intrusive.

Sakai and Tsutsumi (1978) also found that δD values decrease as serpentinization increases; their serpentine values were more than 30 per mil lower with respect to meteoric waters. If-53 per mil approximates the average value of δD for local meteoric waters in the State of Mexico, differences with respect to our lowest (ME-V-4) and highest (ME-V-7) δD values of serpentines range between 32 and 63 per mil; if we adopt the minimum value of -70 per mil suggested by Wenner and Taylor (1974) the range is 15 to 46 per mil for the same samples. Meteoric water is the most likely water type introduced during serpentinization; however, the low δD values in our samples must be explained not only on the basis of water circulation in a hydrothermal convecting regime. The results of Sakai and Tsutsumi (1978) indicate that below 210°C under isotopic exchange equilibrium, serpentinites should be enriched in deuterium relative to fluid. Since the results in both cases (Japan and Mexico) show an opposite behavior, a logical conclusion migh be that serpentinization does not occur in equilibrium with meteoric hydrothermal fluids, or that the exchange waters were isotopically different from modern waters. Sakai and Tsutsumi (1978) propose that formation of lizardite-chrysotile proceeds kinetically rather than in equilibrium, in order to acquire isotopically lighter water.

For some years, the process of serpentinization was related to water availability rather than temperature (Coleman, 1971; Wicks and Whittaker, 1977). In the case of San Pedro Limón, the most serpentinized rocks are closely related to large structures of emplacement, which induced the development of secondary permeability. Fluid participation in fault zones has been isotopically documented by Kerrich *et al* (1984), suggesting that fluid regimes follow a sequence which results from conditions of high temperature and pressure under low water/rock ratios (high ^{18}O) to high fluid fluxes in large scale conditions of permeability as the structures propagate. From chemical and isotopic data in the San Andreas Fault (Irwin and Barnes, 1975; Sibson, 1982), high and low temperature fluid regimes can coexist in deep and shallow levels of the crust. High-temperature regimes (360°-450°C) correspond to metamorphic fluids in shear zones, while relatively low-temperature fluids (200°C) have been reported from the West Bay transcurrent fault in the Yellowknife greenstone belt, where fluids may be meteoric or from original brines (Kerrich *et al,* 1984). The San Andreas and West Bay faults are deep and narrow structures. In contrast, the zone of San Pedro Limón-Palmar Chico belongs to wider and, at least, locally shallower faults which should involve a larger meteoric influence.

The lowering in δD values with respect to increasing serpentinization is explained by Sakai and Tsutsumi (1978) by a mechanism where, as hydration of the ultramafics ad-,
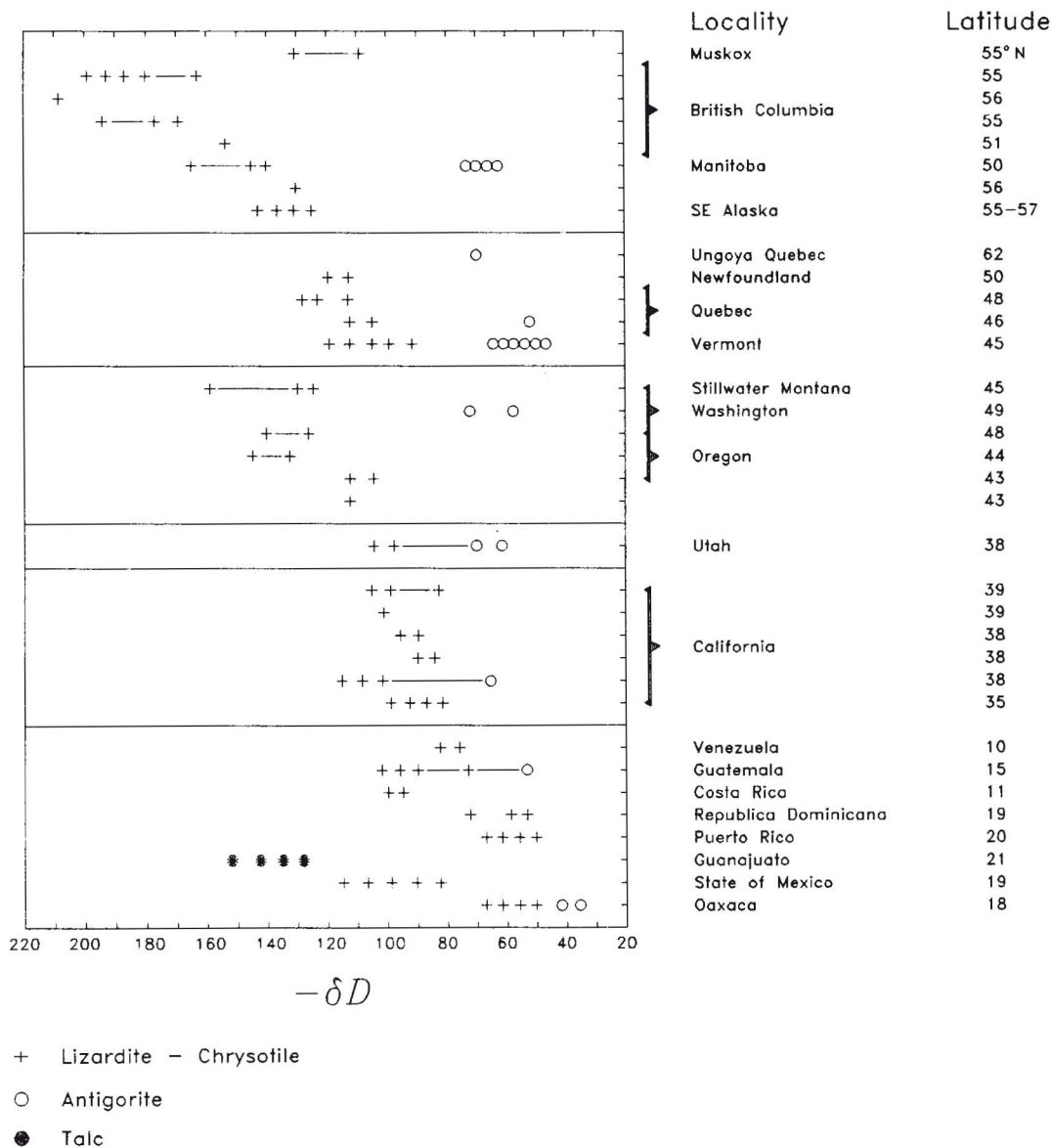
Locality	Latitude
Muskox	55° N
	55
British Columbia	56
	55
	51
Manitoba	50
	56
SE Alaska	55–57
Ungoya Quebec	62
Newfoundland	50
Quebec	48
	46
Vermont	45
Stillwater Montana	45
Washington	49
	48
Oregon	44
	43
	43
Utah	38
	39
	39
	38
California	38
	38
	35
Venezuela	10 N
Guatemala	15
Costa Rica	11
Republica Dominicana	19
Puerto Rico	20
Guanajuato	21
State of Mexico	19
Oaxaca	18

$-\delta D$

+   Lizardite — Chrysotile

○   Antigorite

●   Talc

Fig. 5. Correlation between latitude and δ D of serpentines from the Americas (modified after Wenner and Taylor, 1974). Mexican serpentines from Guanajuato (Delgado-Argote, 1987; talc and serpentine from normal faults), Oaxaca (antigorite and lizardite-chrysotile from the Cuicateco fold and thrust belt (Casar-Alderete *et al.,* 1986) and State of Mexico (this study).

vances through grain boundaries, cracks, and fissures the fluids are progressively enriched in deuterium as protium is incorporated into serpentine. In addition, serpentinization produces alkaline solutions and hydrogen isotope exchange between serpentine, and the remaining water tends to be too slow, allowing the kinetic isotope effect to be preserved even under high rock/water ratios regimes.

Within the uncertainties on the behavior of hydrogen during serpentinization, our results are comparable with δD values reported from serpentinites formed with participation of meteoric waters, and they are in good agreement with the empirical results published so far.

CONCLUSIONS

1. The area of San Pedro Limón-Palmar Chico belongs to an Albian island arc lithologically characterized by a volcanosedimentary andesitic sequence and a sedimentary domain deposited in small basins. In San Pedro Limón, the sedimentary sequence is intruded by a dioritic-peridotitic stock, while small serpentinitic wedges, associated with large structures, do not show clear relationships with respect to other intermediate intrusives. Contact relationship between intrusives and the enclosing sedimentary rocks are mainly tectonic, and do not develop temperature metamorphism. Structural evidence indicates that the emplacement of the ultramafics took place during a Neogene transpressive regional event.

2. Infrared spectra of nine serpentinized rocks indicate the presence of lizardite-chrysotile mixtures, and absence of antigorite was confirmed. Temperature regimes must be
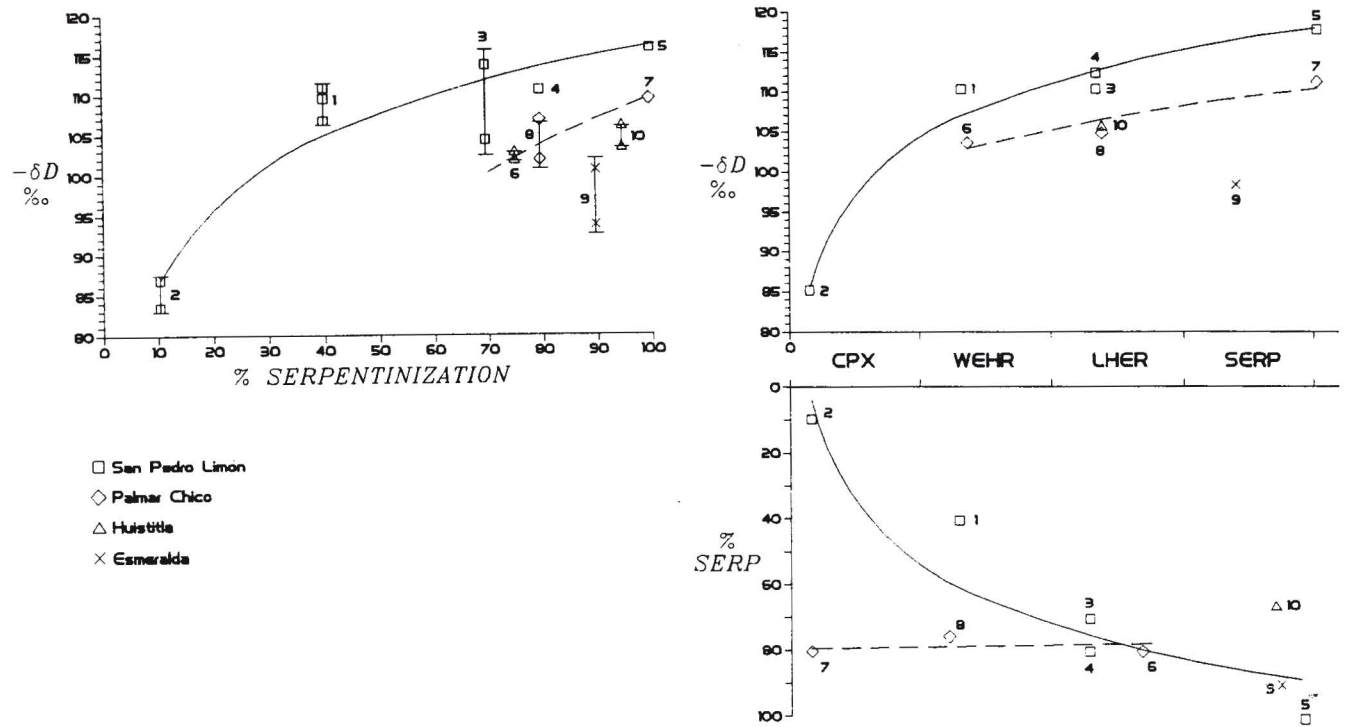
Fig. 6. A. δ D versus estimated volume percent serpentinization. Solid and dashed lines are best-fit lines (logarithmic) of samples from San Pedro Limón and Palmar Chico, respectively. Bars indicate standard deviation. B. Correlation between inferred protolith with respect to average δ D and degree of serpentinization as indicated in Tables 1 and 2. Solid and dashed lines are best-fit lines of samples from San Pedro Limón and Palmar Chico, respectively.

in the range of 100°-200°C, based on the association of lizardite-chrysotile. Some slip-fiber chrysotile was formed under shearing stress during the emplacement of the ultramafic masses.

3. The degree of serpentinization of the ultramafics depends on the proportion of original olivine with respect to pyroxenes, and more serpentinized rocks show lower δD values. The very low δD values (-85 to -116 per mil) of the structural water of serpentines must be attributed to influx of meteoric water during the Neogene disturbance, and may be related to a kinetic effect rather than to a serpentinization under equilibrium with local meteoric water.

BIBLIOGRAPHY

BARNES, I. and J. R. O'NEIL, 1969. The relationship between fluids in some fresh alpine-type ultramafics and possible modern serpentinization, Western United States. *Geol. Soc. Am. Bull., 80,* 1974-1960.

BRINDLEY, G. W. and J. ZUSSMAN, 1959. Infrared absorption data for serpentine minerals. *Am. Mineral., 44,* 185-188.

CASAR-ALDRETE, I., L. A. DELGADO-ARGOTE, P. MORALES-PUENTE and E. L. GONZALEZ-CAVER, 1986. Significado geológico de D/H en agua estructural de serpentinas de Concepción Pápalo, Oaxaca: resultados preliminares. Geos Boletín, época II, Unión Geofísica Mexicana (resúmenes), p.23.

COLEMAN, R.G., 1971. Pretrologic and geophysical nature of serpentinites. *Geol. Soc. Am. Bull., 82,* 897-18.

COX, K.G., J.D. BELL and R.J. PANKHURST, 1979. The interpretation of igneous rocks. George Allen and Unwin, 450 pp.

CRAIG, H., 1961. Standard for reporting concentrations of deuterium and oxygen-18 in natural waters. *Science, 133,* 1833-1934.

DE CSERNA, Z., 1982 (1983). Hoja Tejupilco, 14 Q-g (9), con resúmen de la geología de la Hoja Tejupilco, Estados de Guerrero, México y Morelos: Universidad Nacional Autónoma de México, Instituto de Geología, Carta Geológica de México, Serie de 1:100,000, mapa con texto, 46 pp.

DELGADO-ARGOTE, L.A., 1986. Geology and economic study of ultramafic complexes of the coast of Guerrero, Mexico. M. S. Thesis, University of Arizona, 137 pp.

DELGADO-ARGOTE, L. A., 1987. Efectos estructurales del tronco homblendítico de San Pedro Limón, Edo. de México, en un sistema transpresivo Terciario del terreno Tierra Caliente. Geos Boletín, época II, Unión Geofísica Mexicana (resúmenes), p. 30.

DELGADO-ARGOTE, L. A., 1987. Análisis de D/H en alteraciones de rocas ultramáficas de San Juan de Otates, Guanajuato. Universidad Nacional Autónoma de México, Instituto de Geología, Simposio sobre la Geología de la Región de la Sierra de Guanajuato, Programa, Resúmenes y Guía de Excursión, p. 16-17.

DELGADO-ARGOTE, L. A., 1989. Regional implications of the Jurassic-Cretaceous volcanosedimentary Cuicateco terrane, Oaxaca, Mexico. *Geofís. Int. 28*, 939-974.

DELGADO-ARGOTE, L. A., R. RUBINOVICH-COGAN and A. GASCA-DURAN, 1986. Descripción preliminar de la geología y mecánica de emplazamiento del complejo ultrabásico del Cretácico de Loma Baya, Guerrero. *Geofís. Int. 25*, 537-558.

DELGADO-ARGOTE, L. A., J. MUÑOZ-VELASCO and M. J. ARAGON-ARREOLA, 1988. Ambiente geológico y relaciones petrológicas de las rocas ultramáficas de la secuencia vulcanosedimentaria del área de San Pedro Limón-Palmar Chico, Estado de México. *En:* Universidad Nacional Autónoma de México, Instituto de Geología, Tercer Simposio Geológia Regional de México, Memoria, p. 24-27.

GARCIA-CALDERON, J., 1978. Asbestos de México. *Bol. Soc. Geol. Mex., 39*, 154-161.

GOLIGHTLY, P. and J. N. ARANCIBIA, 1979. The chemical composition and infrared spectrum of nickel and iron-substituted serpentine from a nickeliferous laterite profile, Soroako, Indonesia. *Can. Mineral., 17*, 719-728.

IRWING, W. P. and I. BARNES, 1975. Effects of geologic structure and metamorphic fluids on seismic behaviour of the San Andreas fault system in central and northern California. *Geology, 3*, 713-716.

KERRICH, R., T. E. LA TOUR and L. WILLMORE, 1984. Fluid participation in deep fault zones: evidence from geological, geochemical and 18 O/16 O relations. *J. Geophys. Res., 89*, 4331-4343.

LUCE, R.W., 1971. Identification of serpentine varieties by infrared absorption. United States Geological Survey, Professional Paper 750-B, p. B199-B201.

MAGARITZ, M. and H. P. TAYLOR, JR., 1974. Oxygen and hydrogen isotope studies of serpentinization in the Troodos ophiolite complex, Cyprus. *Earth Planet. Sci. Lett., 23*, 8-14.

ORTEGA-GUTIERREZ, F., 1981. Metamorphic Belts of Southern Mexico and their Tectonic Significance. *Geofís. Int., 20*, 177-202.

PAGE, N. J., 1968. Chemical differences among the serpentine "polymorphs". *Am. Mineral., 53*, 201-215.

PANTOJA-ALOR, J., 1959. Estudio geológico de reconocimiento de la región de Huetamo, Estado de Michoacán. Consejo de Recursos Naturales No Renovables (México), Boletín 50, 36 pp.

PANTOJA-ALOR, J., 1983. Geocronometría del Cretácico-Terciario de la Sierra Madre del Sur. *Bol. Soc. Geol. Mex., 44*, 1-20

SAKAI, H. and M. TSUTSUMI, 1978. D/H fractionation factors between serpentine and water at 100° to 500°C and 2000 bar water pressure, and the D/H ratios of natural serpentines. *Earth Planet. Sci. Lett., 40*, 231-242.

SALAS-CASTELLANOS, J. E., 1982. Geología de la Región de Amatepec y Evaluación Metalogenética del prospecto "La Sierra", Tlatlaya, Estado de México. Tesis Profesional, Facultad de Ingeniería, UNAM, México, 71 pp.

SECRETARIA DE PROGRAMACION Y PRESUPUESTO (CETENAL). Carta de Climas, escala 1:1 000 000. (sin año).

SHEPARD, S. M. F., 1986. Characterization and isotopic variations in natural waters. *In:* Stable isotopes in high temperature geological processes, J. W. Valley, H. P Taylor, Jr., J. R. O'Neil (editors), Reviews in *Mineralogy, 16*, 165-183.

SIBSON, R. H., 1982. Fault zone models, heat flow, and the depth distribution of earthquakes in the continental crust of the United States. *Bull. Seism. Soc. Am., 72*, 151-163.

SYLVESTER, A.G., 1988. Strike-slip faults. *Geol. Soc. Am. Bull., 100*, 1666-1703.

WENNER, D. B. and H. P. TAYLOR, JR., 1973. Oxygen and hydrogen isotope studies of the serpentinization of ultramafic rocks in oceanic environments and continental ophiolite complexes. *Am. J. Sci., 273*, 207-239.

WENNER, D. B. and H. P TAYLOR, JR., 1974. D/H and .O 18/O 16 studies of the serpentinization of ultramafic rocks. *Geochim. Cosmochim. Acta, 38*, 1255-1286.

WICKS, F. J. and E. J. W. WHITTAKER, 1977. Serpentine textures and serpentinization. *Can. Mineral., 15*, 459-488.

YARIV, S. and L. HELLER-KALLAI, 1975. The relationship between the I.R. spectra of serpentines and their structures. *Clays and Clay Minerals, 23*, 145-152.

Delgado-Argote, L.A.[1], I. Casar-Aldrete[2], E. González-Caver[2], P. Morales-Puente[2] and P. Girón-García[3].

1 Instituto de Geología, UNAM., Present Address: División Ciencias de la Tierra, CICESE. 22860, Ensenada, Baja California, México.
2 Instituto de Física, UNAM.
3 Instituto de Geología, UNAM. Del. Coyoacán, 04510, México, D.F. México.